Ceramics-Silikáty 61 (1), 40-44 (2017)
journal webpage: www.ceramics-silikaty.cz doi: 10.13168/cs.2016.0058

COMPACTION OF LITHIUM-SILICATE CERAMICS USING SPARK PLASMA SINTERING

#TOMÁŠ FRANTIŠEK KUBATÍK, FRANTIŠEK LUKÁČ, RADEK MUŠÁLEK, VLASTIMIL BROŽEK, KVĚTA STEHLÍKOVÁ, TOMÁŠ CHRÁSKA

Institute of Plasma Physics CAS, Za Slovankou 1782/3, 182 00 Prague, Czech Republic

#E-mail: kubatik@ipp.cas.cz

Submitted September 2, 2016; accepted October 24, 2016

Keywords: Li_2SiO_3, $Li_2Si_2O_5$, Spark plasma sintering (SPS), Quantitative Rietveld refinement, X-ray diffraction (XRD)

This paper deals with the compaction of ceramics based on lithium-silicate by spark plasma sintering (SPS). The initial powder was prepared by calcination in a resistance furnace at a temperature of 1300°C with the ratio of Li/Si = 1. Compacting by SPS was carried out at temperatures of 800 - 1000°C with a maximum pressure of 80 MPa. Samples with open porosity of less than 1 % were prepared at the temperature of 1000°C. According to the quantitative Rietveld refinement of x-ray diffraction data, the dominant phases in all samples were $Li_2Si_2O_5$ and Li_2SiO_3, together representing over 80 wt. % of the sintered material.

INTRODUCTION

Due to its low thermal expansion, low density and high strength, lithium-silicate ceramics are the object of a still growing number of research works, e.g. [1-10]. Lithium-silicate ceramics have a promising application potential mainly in D-T fusion reactors as a breeder material for tritium production [3, 4]. Besides, it finds use for electronic equipment [1] and in lithium batteries [5, 6]. It was published that lithium ceramic exhibits a very high absorption ability for carbon dioxide CO_2 at higher temperatures [7]. Lithium silicate ceramics is also widely used in dental applications [8]. There are several types of lithium-silicate ceramics depending on the initial ratio of Li/Si; at the ratio of 2 and sintering temperatures of 800 - 900°C, it is possible to prepare 99 % pure Li_2SiO_3, and at the ratio of Li/Si = 4 and temperature of 1230°C, Li_4SiO_4 phase was prepared [9]. Other kinds of lithium-containing ceramics based on $LiAlSiO_4$, $LiAlSi_2O_6$ (LAS) are distinguished by a negative thermal expansion coefficient [10]. Sintering methods such as field assisted sintering (FAST) [11, 12], also known as spark plasma sintering (SPS) or pulsed electric current sintering, as well as the methods of inductive sintering [13], or reactive sintering [14], are unconventional sintering techniques which may be used to provide lithium-silicate ceramics. This paper reports on the preparation via SPS of Li-Si ceramics composed mainly of Li_2SiO_3 and $Li_2Si_2O_5$.

EXPERIMENTAL

The feedstock powder for SPS sample preparation was made by reaction between SiO_2 and Li_2CO_3 powders (p.a., Lachema, Czech Republic) in an electric resistance furnace. The two powders were mixed in a mass ratio of 1/1 (Li/Si), heated in a corundum crucible to 1300°C and kept at the processing temperature for 1 hour. After cooling, the solidified ceramic cast was removed, broken to pieces and ground in a ball-mill at 1100 rpm for 10 minutes (Retsch, Germany). A sieved powder fraction, containing only grains smaller than 120 μm, was used for SPS sample preparation. The powder was compacted by SPS using the SPS 10-4 system (Thermal Technology, USA) with graphite tooling at 800, 900 and 1000°C. Since softening of silicates at higher temperatures is a common phenomenon, two heating steps were set up to prevent tooling damage. First the heating speed was set to 100°C·min^{-1} and the pressure was increased with the speed of 10 MPa·min^{-1} to the resultant 80 MPa until the temperature of 700°C was reached. Then, slow heating at the rate of 20°C·min^{-1} and simultaneous partial relief (50 MPa·min^{-1}) to the final pressure of 5 MPa followed. When the target temperature was reached, the sample was held at the selected temperature for 10 min. Open porosity of the prepared samples of cylindrical shape with a diameter of 20 mm and a height of 3 - 5 mm was measured by the Archimedes method. The microstructure of the polished sections was observed using a scanning

electron microscope EVO MA 15 (Carl Zeiss SMT, Germany, SEM). Ground surfaces of sintered samples were measured in standard Bragg-Brentano geometry of D8 Discover powder X-ray diffractometer (Bruker, Germany) with Cu$K\alpha$ radiation and 1D detector. A beam knife was placed above the surfaces in order to minimize air scattering at lower incident angles. Quantitative phase analysis was done via the Rietveld method using phase entries from the Inorganic Crystal Structure Database (ICSD) using TOPAS V5 (Coelho Software). For 3-point bending, Instron 1362 (Instron, UK) with 14.55 mm span of outer supports was used. Beams with approximately 4 × 4 mm cross-section were prepared with a precision saw and ground and chamfered with P600 SiC paper in order to obtain a smooth surface and planarity of the opposite sides. The samples were loaded with a 0.2 mm·min^{-1} loading rate until sudden fracture occurred. The maximum load was used for the evaluation of flexural strength according to the ASTM C1161 standard.

RESULTS

Densification behaviour

The records of densification by SPS are given in Figures 1 and 2. The graphs show the movement of the upper punch position under the influence of applied pressure, temperature and process time. As an illustration, the sintering schedules are given here for temperatures of 800 and 1000°C (Figure 1 and 2) at which the differences in the sintering processes are clearly apparent.

It can be seen in the graphs in Figure 1 that an almost linear reduction of the sample height occurs in the graphite crucible with increasing temperature and pressure. After attaining the temperature of 700°C, the pressure starts to decrease. Along with the simultaneous gradual increase in temperature, the punch position is again extending up to the preset temperature of 800°C. At approximately 720°C, the target pressure of 5 MPa is reached and then a slow linear displacement of the punch position occurs which reflects their dilatation during heating. There was a very small difference in the nature of the sintering process for 800 and 900°C. However for the samples sintered at 1000°C the graphs in Figure 2 document that at about 930°C softening occurs. Consequently, intense sintering is observed and a significantly lower porosity is obtained for these sintering parameters. The open porosity values in Table 1 clearly show that while the sample sintered at 1000°C has ~1 % porosity, the sintering at the two lower temperatures results in comparatively high porosities exceeding 22 % and 16 % for 800 and 900°C, respectively.

Table 1. Open porosity in dependence of the sintering temperature.

Temperature of sintering (°C)	Open porosity (%)
800°C	22.4
900°C	16.5
1000°C	0.9

Microstructure

Figure 3 shows that the milled powder prepared by calcining of SiO_2 and Li_2CO_3 at 1300°C for 1 h is composed of sharp-edged elongated particles. Significant differences in porosity of the sintered samples are also apparent on the microstructure shown in Figures 4-6. Whereas sintering at 800°C produced material with poorly bonded particles and high porosity level, sintering at 1000°C, taking advantage of softening mechanism in the Li-Si material, leads to a more compact microstructure and better bonding between the individual particles.

Figure 5 shows that during sintering at 900°C individual particles start to connect diffusively and, thus, better particle bonding in comparison to 800°C is

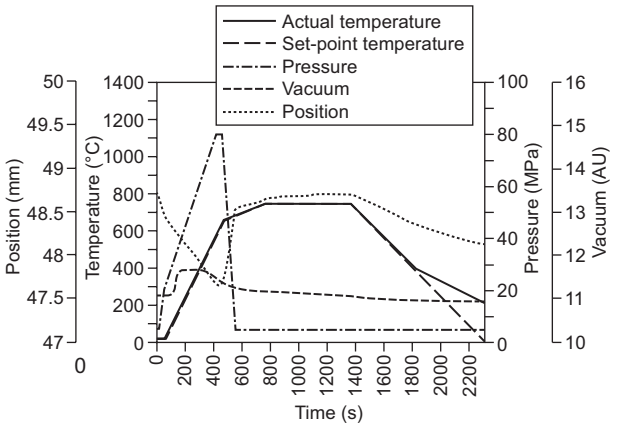

Figure 1. Record of process parameters used for sintering the powder of lithium ceramics at 800°C (SPS).

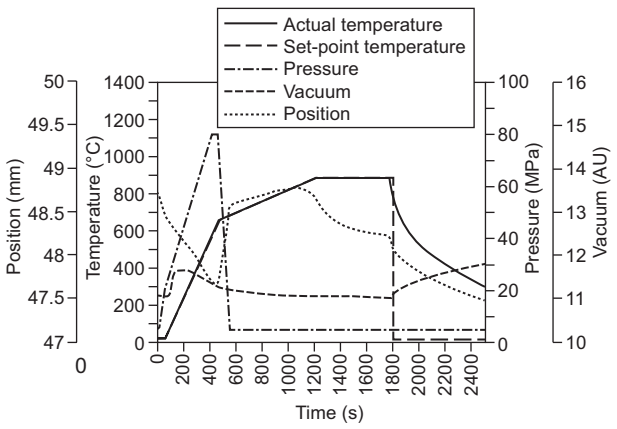

Figure 2. Record of process parameters used for sintering the powder of lithium ceramics at 1000°C (SPS).

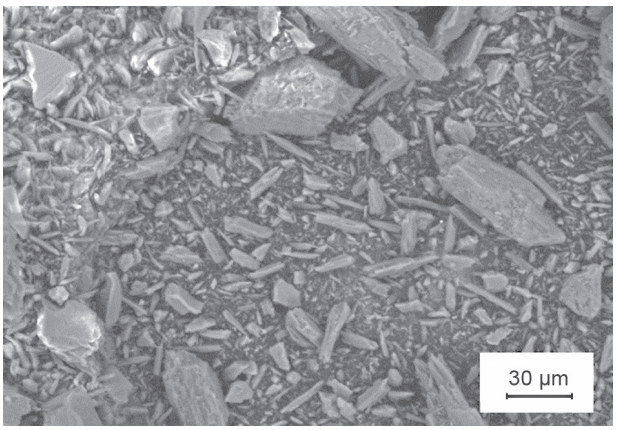

Figure 3. Shape of the powder used for the SPS sintering (SEM-BSE).

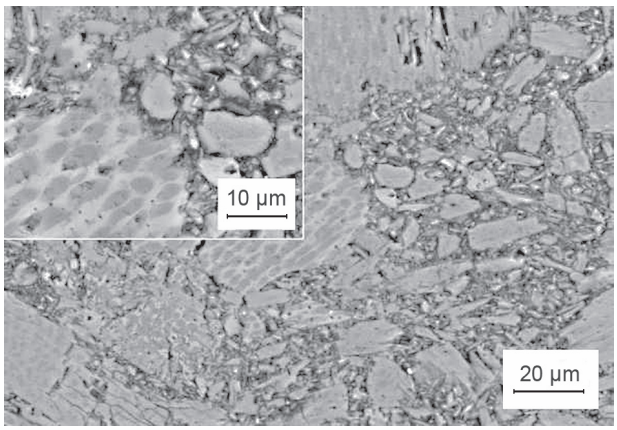

Figure 4. Microstructure of the cross-section of lithium ceramics prepared by SPS at 800°C (SEM-BSE).

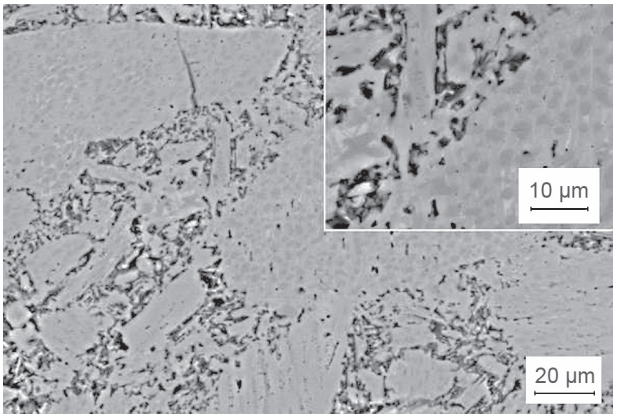

Figure 5. Microstructure of the cross-section of lithium ceramics prepared by SPS at 900°C (SEM-BSE).

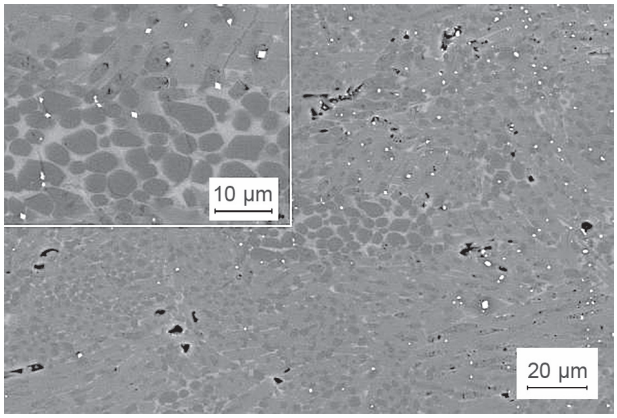

Figure 6. Microstructure of the cross-section of lithium ceramics prepared by SPS at 1000°C (SEM-BSE).

obtained. Since the compactness of the obtained materials has to be considered from the viewpoint of phase miscibility, quantitative phase analysis was also carried out.

Quantitative phase analysis

All the analyzed samples, including the initial powder, are composed dominantly of orthorhombic lithium silicon oxides, namely $Li_2Si_2O_5$ (Ccc2 space group) and Li_2SiO_3 (Cmc21 space group) that form in each case together more than 80 wt. % of the sample mass, with $Li_2Si_2O_5$ being more abundant. There is an evolution of the quantities of these two dominant phases as revealed in Table 2, but it is not dramatic and these two starting phases have been to a large extent preserved during SPS.

In diffractograms of powder and sample sintered at 800°C were found two modifications of alpha-quartz structure caused by different microstructure aspects. Firstly, very broad reflections correspond to particles with small coherently diffracting domains (CDD) i.e. low

Table 2. Results of quantitative Rietveld refinement of samples sintered at 800, 900 and 1000°C (the estimated error is 5 rel. %).

	powder	800°C	900°C	1000°C
Li_2SiO_3	41	40	33	33
$Li_2Si_2O_5$	48	49	57	55
Quartz	3.6	3.0	2.8	0.9
Quartz low CDD	2.8	2.3	–	–
β-spodumene	4.6	5.5	7.7	6.2
virgilite	–	–	–	4.2

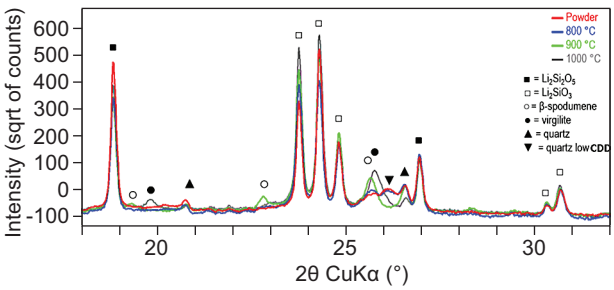

Figure 7. Comparison of powder XRD patterns with phase identification; the range was selected in order to adequate indicate the presence of the minor phase reflections.

crystallites size of alpha-quartz denoted as "quartz low CDD". Secondly, higher crystallites size of other alpha-Quartz structure particles produced sharp reflections. Therefore, fitting procedure included two phases of one crystallographic structure with slightly different lattice parameters.

The main differences are in the presence of minor phases as depicted in Figure 7. Most prominently, we observe lower intensity of quartz reflections, i.e. (010) and (101) with triangles above in Figure 7, in the 1000°C sample and the occurrence of new reflections which belong to a LAS phase called virgilite [15]. Thus, we assume that virgilite was created by reaction of silicon ions from quartz with the lithium rich phases. Nevertheless, virgilite is not the only lithium aluminium silicate in the material, since the very powder included so-called β-spodumene $LiAl(SiO_3)_2$ or high temperature LAS phase. Its presence remains rather stable, about 5 wt. %, except for the 900°C sample, which has about 8 wt. % of β-spodumene. The reason of the existence of LAS is most probably the annealing of the starting powder in the corundum crucible. The results of Rietveld refinement are shown in Figure 8 and reflect a fairly good agreement between the measured data (blue points) and the obtained fits (red patterns).

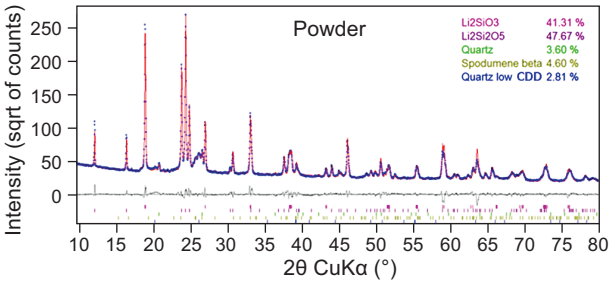

a)

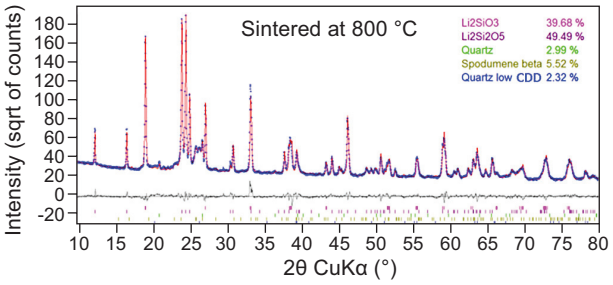

b)

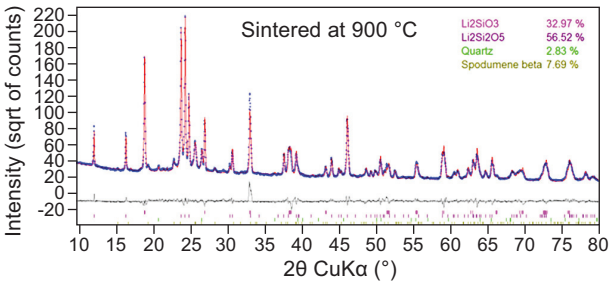

c)

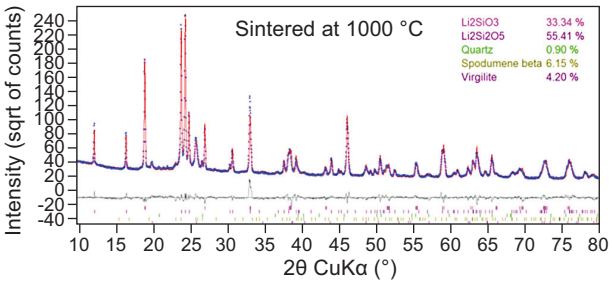

d)

Figure 8. Results of quantitative Rietveld refinements.

Three-point flexural strength

For all tested samples, brittle behavior was observed. Average values of 3-point bending results are represented in the graph in Figure 9. It shows a clearly evident influence of the sintering temperature on the flexural strength. A flexural strength of 20.9 MPa is attained for samples sintered at 800°C. After sintering at 900°C, diffusion bonds by necks occur, which is evident from the microstructure observation and also from the higher strength of 69.2 MPa, which is achieved for these samples. Porosity decreased down to 0.9 % for the sintering temperature of 1000°C and significant diffusion occurred, resulting in the creation of a compact microstructure with a resultant strength of 154.1 MPa, which is almost 8 times higher than for sample sintered at 800°C.

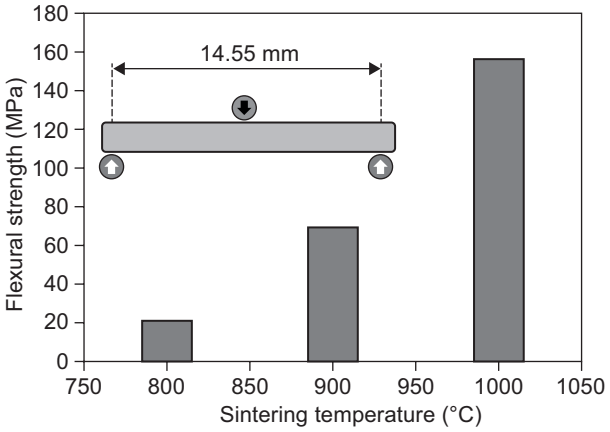

Figure 9. Results of three-point bending strength tests of samples sintered at 800, 900 and 1000°C, respectively.

CONCLUSION

In this paper, samples of lithium-silica ceramics were prepared by the Spark Plasma Sintering method. Using a suitably selected program, compacting even above the softening temperature was carried out. The

porosity of the prepared samples is greatly dependent on the sintering temperature. The values of open porosity are 22.4 % for the temperature of 800°C, 16.5 % for 900°C and a sample with open porosity of 0.9 % was prepared at the temperature of 1000°C for 10 min with pressure of 5 MPa. Necks, which are indicative of diffusion processes during sintering, were observed in the microstructure at the temperature of 900°C. The sintering process did not lead to pronounced changes in the phase composition with orthorhombic $Li_2Si_2O_5$ and Li_2SiO_3, forming over 80 wt. % in all cases. The main evolution of phases included silica and LAS phases, with virgilite created in the sample sintered at the highest temperature. The influence of increasing sintering temperatures is evident for three-point bending (flexural) strength. A strength of 20.9 MPa was attained for samples sintered at 800°C, 69.2 MPa for samples sintered at 900°C and 154.1 MPa for samples sintered at 1000°C.

Acknowledgements

The authors would like to thank Zdenek Pala from the University of Nottingham, UK, for fruitful discussions about quantitative phase composition and Rietveld refinement issues.

The work was supported by the Grant Agency of the Czech Republic through the project number 14-36566G entitled Multidisciplinary research centre for advanced materials.

REFERENCES

1. Prasad A., Basu A. (2012): Structural and dielectric studies of Li_2SiO_3 ceramic. *Materials Letters, 66,* 1-3. doi:10.1016/j.matlet.2011.08.055
2. Cruz D., Bulbulian S., Lima E., Pfeiffer H. (2006): Kinetic analysis of the thermal stability of lithium silicates (Li_4SiO_4 and Li_2SiO_3). *Journal of Solid State Chemistry, 179,* 909-916. doi:10.1016/j.jssc.2005.12.020
3. Van der Laan J.G., Fedorov A.V., Van Til S., Reimann J. (2012): 4.15 -Ceramic Breeder Materials. *Comprehensive Nuclear Materials, 4,* 463-510. doi: 10.1016/B978-0-08-056033-5.00114-2
4. Gao X., Chen X., Gu M., Xiao Ch., Pen S. (2012): Fabrication and characterization of Li_4SiO_4 ceramic pebbles by wet method. *Journal of Nuclear Materials, 424,* 210-215. doi:10.1016/j.jnucmat.2012.02.018
5. Zhang S., Deng C., Gao H., Meng F.L., Zhang M. (2013): $Li_{2+x}Mn_{1-x}P_xSi_{1-x}O_4/C$ as novel cathode materials for lithium ion batteries. *Electrochimica Acta, 10,* 406-412. doi: 10.1016/j.electacta.2013.06.064
6. Shao B., Taniguch I. (2012): Synthesis of Li_2FeSiO_4/C nanocomposite cathodes for lithium batteries by a novel synthesis route and their electrochemical properties. *Journal of Power Sources, 199,* 278-286. doi:10.1016/j.jpowsour.2011.10.050
7. Chowdhury M. B.I., Quddus M. R., De Lasa H. I. (2013): CO_2 capture with a novel solid fluidizable sorbent: Thermodynamics and Temperature Programmed Carbonation–Decarbonation. *Chemical Engineering Journal, 23,* 139-148. doi:10.1016/j.cej.2013.07.044
8. Gohin C. B., Duval J. L., Azogui E. E., Jannetta R., Pezron I., Maquin D. L., Gangloff S.C., Egles C. (2013): Soft tissue adhesion of polished versus glazed lithium disilicate ceramic for dental applications. *Dental Materials, 29,* 205-212. doi:10.1016/j.dental.2013.05.004
9. Tang T., Zhang Z., Meng J. B., Luo D. L. (2009): Synthesis and characterization of lithium silicate powders. *Fusion Engineering and Design, 84,* 2124-2130. doi:10.1016/j.fusengdes.2009.02.017
10. Moreno O. G., Borrell A., Bittmann B., Fernández A., Torrecillas R. (2011): Alumina reinforced eucryptite ceramics: Very low thermal expansion material with improved mechanical properties. *Journal of the European Ceramic Society, 31,* 1641-1648. doi:10.1016/j.jeurceramsoc.2011.03.033
11. Vanmeensel K., Laptev A., Hennicke J., Vleugels J., Biest O. (2005): Modelling of the temperature distribution during field assisted sintering. *Acta Materialia, 53,* 4379–4388. doi:10.1016/j.actamat.2005.05.042
12. Kubatík F.T., Pala Z., Novák P. (2015): Compacting the powder of Al-Cr-Mn Alloy with SPS. *Materials and Technology, 49,* 129-132.
13. Zhang J., Zavaliangos A., Groza Jr. J. (2003): Field activated sintering techniques: a comparison and contrast. *P/M Science and Technology Briefs, 5,* 17–21.
14. Novák P., Marek I., Mejzlíková L., Michalcová A., Vojtěch D. (2012): Reactive-sintering production of intermetallic. *Materials and Technology, 46,* 559-562.
15. Jezek P.A., Appleman D.E. (1978): Virgilite: a new lithium aluminum silicate mineral from the Macusani glass, Peru. *American Mineralogist, 63,* 461-465.